

Ehrenfest Modeling of Cavity Vacuum Fluctuations and How to Achieve Emission from a Three-Level Atom

Ming-Hsiu Hsieh,¹ Alex Krotz,¹ and Roel Tempelaar^{1, a)}

Department of Chemistry, Northwestern University, 2145 Sheridan Road, Evanston, Illinois 60208, USA

A much-needed solution for the efficient modeling of strong coupling between matter and optical cavity modes is offered by mean-field mixed quantum–classical dynamics, where a classical cavity field interacts self-consistently with quantum states of matter through Ehrenfest’s theorem. We previously introduced a modified mean-field approach, referred to as decoupled mean-field (DC-MF) dynamics, wherein vacuum fluctuations of the cavity field are decoupled from the quantum-mechanical ground state as a means to resolve an unphysical drawing of energy from the vacuum fluctuations by a two-level atom. Here, we generalize DC-MF dynamics for an arbitrary number of (nondegenerate) atomic levels, and show that it resolves an unphysical lack of emission from a three-level atom predicted by conventional mean-field dynamics. We furthermore show DC-MF to provide an improved description of reabsorption and two-photon emission processes.

In recent years, strong light–matter coupling has come under increased scrutiny as a viable means to modify the physical and chemical properties of matter.^{1–10} Coupling atoms, molecules, and materials to confined optical modes inside cavities gives rise to hybrid light–matter excitations called polaritons, which have experimentally been demonstrated to impact chemical reactions,^{11–14} energy transfer,^{15–19} and other phenomena. However, the basic principles governing such polaritonic effects remain debated. In order to further unravel such principles, there is a particular need for theoretical models that realistically capture cavity fields beyond the commonly-adopted single-mode representation.^{20,21} For decades, classical dynamics has proven to provide an inexpensive yet accurate means to realistically describe optical fields and their interaction with matter, in the form of finite-difference time-domain²² and finite element methods^{23,24} where matter is accounted for by means of a dielectric. Such approaches have also been combined with quantum master equations in order to phenomenologically account for the quantum-mechanical behavior of matter.^{25–27} Only in recent years, however, has there been significant effort in developing a fully self-consistent mixed quantum–classical framework for the modeling of matter embedded in cavity.^{28–33} It has been shown that the self-consistent interaction between classical light and quantum matter is preferably described through Ehrenfest’s theorem,³¹ employing a mean-field (MF) approximation for the quantum force acting on the classical coordinates.

In spite of its success, such MF modeling has its shortcomings. Perhaps most notably, it suffers from an unphysical transfer of energy out of cavity vacuum fluctuations. The reason for this behavior is that vacuum fluctuations described by classical dynamics are not automatically kept from donating energy, as is the case when describing such fluctuations in terms of quantum-mechanical Fock states. Recently,³⁴ we highlighted this issue for a two-level atom inside a cavity. When prepared in its lower level, the atom was shown to absorb energy out of the cavity vacuum fluctuations, giving rise to “negative” wavefronts in the cavity field emanating from

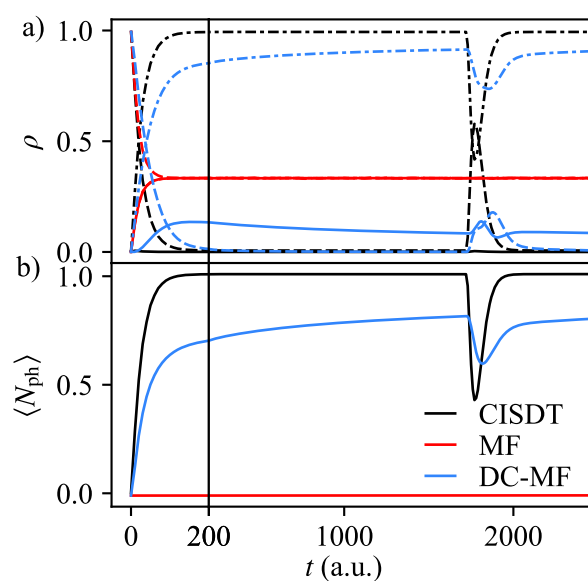


FIG. 1. a) Atomic populations and b) cavity photon number of a symmetric three-level atom initiated in its middle level. Shown are results calculated with CISDT (black), MF dynamics (red), and DC-MF dynamics (blue). Atomic populations are shown for the highest level (solid), middle level (dashed), and lowest level (dash-dotted). The time axis is broken into shorter and longer times for ease of demonstration.

the atom, concomitant with the atom attaining a population in its higher level. Moreover, we introduced a modified MF method wherein vacuum fluctuations are represented by separate classical coordinates which are explicitly decoupled from the lower level of the atom.³⁴ The resulting method, referred to as decoupled mean-field (DC-MF) dynamics, was shown to yield results with radical improvements in accuracy over traditional MF modeling, in addition to rigorously resolving the drawing of energy out of vacuum fluctuations.³⁴

In the present article, we generalize DC-MF dynamics to the case of an arbitrary number of (nondegenerate) atomic lev-

^{a)}Electronic mail: roel.tempelaar@northwestern.edu

els, and apply it to a three-level atom inside a Fabry–Pérot cavity. In doing so, we uncover further manifestations of the shortcomings of the conventional implementation of MF dynamics. In particular, we show that a three-level atom with equal transition energies and transition dipoles between subsequent levels (referred to as a “symmetric” three-level atom) will not emit when initiated in its middle level, but instead will distribute excitation energy among all three levels without exchanging energy with the cavity field, as demonstrated in Fig. 1. The complete lack of emission can be qualitatively understood based on the upward transition yielding negative wavefronts (as found previously³⁴) that cancel out against the positive wavefronts produced by the downward transition. The DC-MF method, by decoupling upward transitions from vacuum fluctuations, resolves this unphysical behavior while consistently providing significant improvements in accuracy.

We consider a multi-level atom described by the Hamiltonian

$$\hat{H}_A = \sum_k \epsilon_k |k\rangle\langle k|, \quad (1)$$

where k runs over the atomic levels, and where the associated energies are denoted ϵ_k . The atomic levels are assumed to be nondegenerate, and ordered such that $\epsilon_k < \epsilon_l$ for any $k < l$. In the conventional implementation of MF dynamics,³⁰ the interaction between the atom and the cavity field is described by the Hamiltonian³⁵

$$\hat{H}_{AF} = \sum_{\alpha} \sum_{k < l} \omega_{\alpha} \lambda_{\alpha} \mu_{kl} Q_{\alpha} |k\rangle\langle l| + \text{H.c.}, \quad (2)$$

where α labels the cavity mode, and with $\omega_{\alpha} = \pi c_0 \alpha L^{-1}$ the associated mode frequency, where c_0 and L are the speed of light and the cavity length, respectively. The classical coordinate Q_{α} represents the electric field amplitude of cavity mode α , while $\mu_{k,l}$ denotes the transition dipole moment between atomic levels k and l . Here, it is assumed that all atomic transition dipoles are aligned with the optical polarization direction. The classical coordinates are treated as harmonic oscillators, governed by the Hamiltonian function

$$H_F = \frac{1}{2} \sum_{\alpha} (P_{\alpha}^2 + \omega_{\alpha}^2 Q_{\alpha}^2), \quad (3)$$

with the momentum-like coordinate P_{α} being associated with the magnetic component of mode α .³⁶

From Eq. 2 it is evident that the interaction between the atom and the cavity field vanishes in the absence of fluctuations of Q_{α} . Such fluctuations may arise due to external pumping of the cavity field or due to thermal motion. In the absence of external pumping, and at low temperatures, the dominant source is vacuum fluctuations instead. Within the conventional implementation of MF dynamics,³⁰ this is accounted for by sampling the classical coordinates from a Wigner distribution, yielding finite fluctuations even in the limit of vanishing temperature. The subsequent dynamics of Q_{α} and P_{α} is governed by Hamilton’s equations of motion, which represent a mode-resolved form of Maxwell’s equations, and which involve a “feedback” force due to the quantum state of the atom,

given by

$$F_{\alpha} = -\langle \psi | \nabla_{Q_{\alpha}} \hat{H}_{AF} | \psi \rangle. \quad (4)$$

The quantum state is expanded in terms of the energy levels as

$$|\psi\rangle = \sum_k c_k |k\rangle. \quad (5)$$

Its time evolution is governed by the time-dependent Schrödinger equation,

$$|\dot{\psi}\rangle = -\frac{i}{\hbar} (\hat{H}_A + \hat{H}_{AF}) |\psi\rangle. \quad (6)$$

Substitution of Eqs. 2 and 5 into Eq. 4 yields

$$F_{\alpha} = -\omega_{\alpha} \lambda_{\alpha} \sum_{k,l} c_k^* c_l \mu_{kl}. \quad (7)$$

When considering a symmetric three-level atom, with equal transition energies and dipoles between subsequent levels, we have $\mu_{12} = \mu_{23} = \mu$, $\mu_{13} = 0$, $\epsilon_1 = -\epsilon_3 = -\epsilon$, and $\epsilon_2 = 0$. Upon initiating the atom in its middle level, $c_2 = 1$, and $c_1 = c_3 = 0$. (Here, we arbitrarily associate the zero point of energy with the middle level and c_2 with the real gauge, which does not affect the outcome of our analysis.) After a time increment Δt , sufficiently short so that the classical coordinates can be assumed to be invariable, the expansion coefficients to second order in Δt are given by

$$\begin{aligned} c_1 &= -c_3^* = -\frac{(\Delta t)^2}{2\hbar^2} \epsilon \Gamma - \frac{i\Delta t}{\hbar} \Gamma \\ c_2 &= 1 + \frac{(\Delta t)^2}{\hbar^2} \Gamma^2, \end{aligned} \quad (8)$$

with $\Gamma \equiv \mu \sum_{\alpha} \omega_{\alpha} \lambda_{\alpha} Q_{\alpha}$. This implies that the middle level is antisymmetrically coupled to the lowest and highest levels, respectively. It is straightforward to verify that $c_1 = -c_3^*$ continues to hold at all times while c_2 remains real-valued. In accordance with Eq. 7, this in turn yields $F_{\alpha} = 0$. The complete absence of any feedback force prevents the atom from donating energy to the cavity field, explaining the lack of emission observed for MF dynamics in Fig. 1.

DC-MF,³⁴ rather than sampling the classical coordinates from a Wigner distribution, represents vacuum fluctuations by a distinct set of coordinates that are drawn from a Gaussian distribution resembling the ground state wave function of the cavity field in Wigner phase-space, and which complements another set representative of thermal fluctuations that are drawn from a Boltzmann distribution. It was first introduced for a two-level atom, for which vacuum fluctuations were explicitly decoupled from the lowest level of the atom, as a pragmatic means to avoid the aforementioned drawing of energy by the atom. Here, we generalize DC-MF by decoupling vacuum fluctuations from the lowest of the involved levels *for every transition* contributing to the atom–field Hamiltonian. Accordingly, Eq. 2 is replaced by

$$\hat{H}_{AF}^{\text{DC}} = \sum_{\alpha} \sum_{k < l} \omega_{\alpha} \lambda_{\alpha} \mu_{kl} (Q_{\alpha} + \rho_l \tilde{Q}_{\alpha}) |k\rangle\langle l| + \text{H.c.} \quad (9)$$

Here, \tilde{Q}_α represents the vacuum fluctuations whereas Q_α represents the thermal fluctuations, each of which are governed by their own set of Hamilton's equations of motion, and involving their own feedback forces.³⁴ Furthermore, $\rho_l \equiv |c_l|^2$ is the quantum population of level l , the inclusion of which gives rise to the aforementioned decoupling.

With regard to the symmetric three-level atom, it is the introduction of the term ρ_l in Eq. 9 that breaks the antisymmetry of the couplings between the middle level and the upper/lower level, as a result of which $c_1 \neq -c_3^*$, and $F_\alpha \neq 0$. This in turn implies that DC-MF allows for emission from a symmetric three-level atom when prepared in the middle level, as further discussed below.

It should be noted that the DC-MF formalism as outlined in the above does not rigorously conserve total energy, unless the time-dependence of the atomic population (ρ_l) can be expressed as a dependence on the classical coordinates, which is nontrivial.³⁴ In the present study, deviations of the total energy are within 2% of the energy transferred between the quantum and classical subsystems.

The calculations presented in this work invoke a single atom located at the center of the cavity. Accordingly, the coupling strength between the atom and the cavity field is given by

$$\lambda_\alpha = \sqrt{\frac{2}{\epsilon_0 L}} \sin\left(\frac{\pi\alpha}{2}\right), \quad (10)$$

where ϵ_0 is the vacuum permittivity. Our parametrization is based on previous work by Hoffmann *et al.*,³⁰ which considered a three-level atom consisting of the lowest three levels of one-dimensional hydrogen.³⁷ However, we modified the transition dipole moments and transition energies associated with the third level in order to produce the symmetric atom from Fig. 1, and to generally assure convergence of the numerically-exact reference calculations (as discussed below). As before,^{30,34} the cavity length was set to $L = 2.362 \times 10^5$ a.u. = 12.5 μm , and the cavity field is represented by its 400 lowest modes, each of which was initiated at zero temperature. For MF and DC-MF dynamics, all observables shown were obtained through the procedure described previously,³⁴ while taking an average over 10^5 trajectories.

The numerically-exact reference calculations involved configuration interaction singles, doubles, and triples (CISDT), while convergence was assured through a comparison with configuration interaction without triples. We note that an inclusion of triples is unnecessary when assuring convergence for a three-level atom initiated in its highest level,³⁰ but that an initiation in the middle level renders convergence much more challenging.

The symmetric three-level atom from Fig. 1 was parametrized as $\epsilon_1 = -0.6738$ a.u., $\epsilon_2 = -0.2798$ a.u., $\epsilon_3 = 0.1142$ a.u. (yielding equal gaps between subsequent levels), and $\mu_{12} = \mu_{23} = 1.034$ a.u. (and with $\mu_{13} = 0$ a.u.), and was initiated in the middle level. As noted before, within MF dynamics the atom redistributes its excitation energy between all three levels. Throughout this process, the photon number is invariably zero, implying a complete lack of emission into the cavity, as rationalized by the antisymmetric couplings

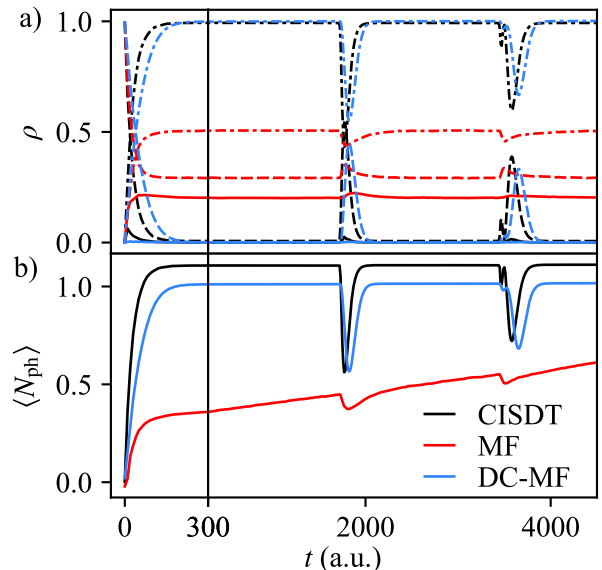


FIG. 2. Same as Fig. 1 but for a three-level atom resembling one-dimensional hydrogen initialized in its middle level.

between the middle level and the lowest and highest levels, respectively.

DC-MF, on the other hand, by breaking the antisymmetry among the inter-level couplings, resolves the unphysical lack of emission by the symmetric three-level atom, yielding a substantial photon number, as shown in Fig. 1. Perhaps more surprisingly, it yields substantial improvements in overall accuracy, generating results in reasonable agreement with the reference calculations. Most notably, it reproduces a complete depletion of the middle level. It also reproduces the reabsorption event arising from optical wavefronts reappearing at the atomic location after cycling through the cavity, although the magnitude of this effect is underestimated. Perhaps the most obvious shortcoming of DC-MF is that it predicts a finite – albeit modest – population of the highest level not seen in the reference calculations.

We now proceed to consider a three-level atom more closely resembling one-dimensional hydrogen, initiated in its second and third levels, adopting the parameters $\epsilon_1 = -0.6738$ a.u., $\epsilon_2 = -0.2798$ a.u., $\epsilon_3 = -0.1547$ a.u., $\mu_{12} = 1.034$ a.u., and $\mu_{23} = -1.5$ a.u. (and with $\mu_{13} = 0$ a.u.). Note that μ_{23} has been adjusted compared to the standard one-dimensional hydrogen values,³⁷ which was necessary in order to assure convergence of the reference calculations for the particular case when the atom is initiated in its middle level.

Shown in Fig. 2 are results for the quasi-hydrogenic three-level atom initiated in its middle level. This level is no longer antisymmetrically coupled to the lowest and highest levels, respectively, even within MF dynamics, due to the parametrization of the atom. Indeed, for MF dynamics we observe a transient rise in the photon number, implying emission of the atom into the cavity field. However, this emission is still severely underestimated by MF dynamics, which generally remains

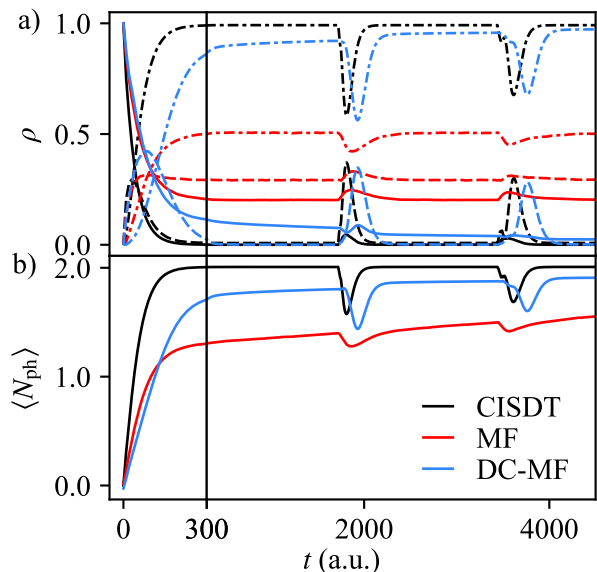


FIG. 3. Same as Fig. 1 but for a three-level atom resembling one-dimensional hydrogen initialized in its highest level.

lacking in quantitative accuracy. In particular, it yields finite asymptotic populations of the middle and highest levels not seen in the reference calculations. DC-MF dynamics, on the other hand, reaches near-quantitative accuracy, including vanishing populations of the middle and highest levels, while capturing the full extent of the reabsorption events. The breaking of the resonance between the lowest-to-middle and middle-to-highest transitions suppresses pathways towards the highest level, as a result of which DC-MF dynamics and the reference calculations resemble the two-level atom results from our previous work.³⁴

Results for the quasi-hydrogenic three-level atom initiated in its highest level are shown in Fig. 3. This case closely resembles the scenario considered previously by Hoffmann *et al.*,³⁰ and represents a two-photon emission process whereby a transient population of the lowest level is accompanied by a population rise and fall of the middle level. MF dynamics was previously seen to capture the rise, but not the fall, of the middle level,³⁰ which is confirmed by Fig. 3. DC-MF dynamics radically improves upon this behavior, once more yielding significant enhancements in accuracy, although it noticeably underestimates the rate of the two-photon emission process.

To summarize, we have presented a generalization of DC-MF dynamics to the case of an arbitrary number of atomic levels. This generalization relies on a decoupling of upward transitions from vacuum fluctuations of the optical field. We have applied the resulting approach to the case of a three-level atom embedded in a Fabry–Pérot cavity, and have shown that it resolves the unphysical lack of emission from a symmetric three-level atom initiated in its middle level predicted by (conventional) MF dynamics. It furthermore leads to remarkable improvements in accuracy when compared to numerically-exact results, capturing reabsorption events as well as two-

photon emission.

Moving forward it will be of interest to assess the accuracy of DC-MF dynamics for cavity-embedded atoms, molecules, and materials beyond three-levels representations. Seeing that configuration interaction becomes computationally prohibitive for such cases, this prompts the need for alternative numerically-exact methods with improved scalability. It should furthermore be noted that the appearance of quantum populations in the atom–field Hamiltonian, as embodied by Eq. 9, can be regarded as a functional dependence of the Hamiltonian on the quantum state. Although it can be argued that the currently-applied “functional” represents the most straightforward choice, exploring alternative functionals may open opportunities to further improve the quantitative accuracy of DC-MF dynamics. It will be of particular interest to consider degenerate levels, and how to best incorporate these into a DC-MF scheme. As things stand, this approach seems to offer a rather promising route towards the merging of classical field descriptions and quantum models of matter, with the potential to bridge between established techniques from both realms, including finite-difference time domain and density functional theory, respectively. We therefore anticipate exciting further developments in the near future.

ACKNOWLEDGEMENT

This work was supported by the National Science Foundation’s MRSEC program (DMR-1720319) at the Materials Research Center of Northwestern University. M.-H.H. gratefully acknowledges support from the Ryan Fellowship and the International Institute for Nanotechnology at Northwestern University. The authors thank Norah Hoffmann for helpful discussions.

- ¹T. W. Ebbesen, *Acc. Chem. Res.* **49**, 2403 (2016).
- ²D. G. Baranov, M. Wersäll, J. Cuadra, T. J. Antosiewicz, and T. Shegai, *ACS Photonics* **5**, 24 (2018).
- ³R. F. Ribeiro, L. A. Martínez-Martínez, M. Du, J. Campos-Gonzalez-Angulo, and J. Yuen-Zhou, *Chem. Sci.* **9**, 6325 (2018).
- ⁴J. Flick, N. Rivera, and P. Narang, *Nanophotonics* **7**, 1479 (2018).
- ⁵M. Hertzog, M. Wang, J. Mony, and K. Börjesson, *Chem. Soc. Rev.* **48**, 937 (2019).
- ⁶J. Keeling and S. Kéna-Cohen, *Annu. Rev. Phys. Chem.* **71**, 435 (2020).
- ⁷K. Nagarajan, A. Thomas, and T. W. Ebbesen, *J. Am. Chem. Soc.* **143**, 16877 (2021).
- ⁸H. Hübener, U. De Giovannini, C. Schäfer, J. Andberger, M. Ruggenthaler, J. Faist, and A. Rubio, *Nat. Mater.* **20**, 438 (2021).
- ⁹A. D. Dunkelberger, B. S. Simpkins, I. Vurgaftman, and J. C. Owrutsky, *Annu. Rev. Phys. Chem.* **73**, 429 (2022).
- ¹⁰T. E. Li, B. Cui, J. E. Subotnik, and A. Nitzan, *Annu. Rev. Phys. Chem.* **73**, 43 (2022).
- ¹¹A. Thomas, J. George, A. Shalabney, M. Dryzhakov, S. J. Varma, J. Moran, T. Chervy, X. Zhong, E. Devaux, C. Genet, J. A. Hutchison, and T. W. Ebbesen, *Angew. Chem. Int. Ed.* **55**, 11462 (2016).
- ¹²R. M. A. Vergauwe, A. Thomas, K. Nagarajan, A. Shalabney, J. George, T. Chervy, M. Seidel, E. Devaux, V. Torbeev, and T. W. Ebbesen, *Angew. Chem. Int. Ed.* **58**, 15324 (2019).
- ¹³A. Thomas, L. Lethuillier-Karl, K. Nagarajan, R. M. A. Vergauwe, J. George, T. Chervy, A. Shalabney, E. Devaux, C. Genet, J. Moran, and T. W. Ebbesen, *Science* **363**, 615 (2019).
- ¹⁴K. Hirai, R. Takeda, J. A. Hutchison, and H. Uji-i, *Angew. Chem. Int. Ed.* **59**, 5332 (2020).

- ¹⁵D. M. Coles, N. Somaschi, P. Michetti, C. Clark, P. G. Lagoudakis, P. G. Savvidis, and D. G. Lidzey, *Nat. Mater.* **13**, 712 (2014).
- ¹⁶X. Zhong, T. Chervy, S. Wang, J. George, A. Thomas, J. A. Hutchison, E. Devaux, C. Genet, and T. W. Ebbesen, *Angew. Chem. Int. Ed.* **55**, 6202 (2016).
- ¹⁷K. Georgiou, R. Jayaprakash, A. Othonos, and D. G. Lidzey, *Angew. Chem. Int. Ed.* **60**, 16661 (2021).
- ¹⁸G. G. Rozenman, K. Akulov, A. Golombek, and T. Schwartz, *ACS Photonics* **5**, 105 (2018).
- ¹⁹R. Pandya, A. Ashoka, K. Georgiou, J. Sung, R. Jayaprakash, S. Renken, L. Gai, Z. Shen, A. Rao, and A. J. Musser, *Adv. Sci.* **9**, 2105569 (2022).
- ²⁰D. S. Wang and S. F. Yelin, *ACS Photonics* **8**, 2818 (2021).
- ²¹J. Fregoni, F. J. Garcia-Vidal, and J. Feist, *ACS Photonics* **9**, 1096 (2022).
- ²²K. Yee, *IEEE Trans. Antennas Propag.* **14**, 302 (1966).
- ²³A. Hrennikoff, *J. Appl. Mech.* **8**, A169 (1941).
- ²⁴R. Courant, *Bull. Amer. Math. Soc.* **49**, 1 (1943).
- ²⁵A. Nagra and R. York, *IEEE Trans. Antennas Propag.* **46**, 334 (1998).
- ²⁶S.-H. Chang and A. Taflove, *Opt. Express* **12**, 3827 (2004).
- ²⁷W. Zhou, M. Dridi, J. Y. Suh, C. H. Kim, D. T. Co, M. R. Wasielewski, G. C. Schatz, and T. W. Odom, *Nature nanotechnology* **8**, 506 (2013).
- ²⁸T. E. Li, A. Nitzan, M. Sukharev, T. Martinez, H.-T. Chen, and J. E. Subotnik, *Phys. Rev. A* **97**, 032105 (2018).
- ²⁹H.-T. Chen, T. E. Li, M. Sukharev, A. Nitzan, and J. E. Subotnik, *J. Chem. Phys.* **150**, 044102 (2019).
- ³⁰N. M. Hoffmann, C. Schäfer, A. Rubio, A. Kelly, and H. Appel, *Phys. Rev. A* **99**, 063819 (2019).
- ³¹N. M. Hoffmann, C. Schäfer, N. Säkkinen, A. Rubio, H. Appel, and A. Kelly, *J. Chem. Phys.* **151**, 244113 (2019).
- ³²T. E. Li, H.-T. Chen, A. Nitzan, and J. E. Subotnik, *Phys. Rev. A* **101**, 033831 (2020).
- ³³M. A. C. Saller, A. Kelly, and E. Geva, *J. Phys. Chem. Lett.* **12**, 3163 (2021).
- ³⁴M.-H. Hsieh, A. Krotz, and R. Tempelaar, *J. Phys. Chem. Lett.* **14**, 1253 (2023).
- ³⁵For simplicity, we omitted the self-polarization term here as well as in Eq. 9, as it only contributes negligibly to the dynamics shown. It should be noted that in some cases, the inclusion of self-polarization term is necessary,^{38–40} and adding this term is straightforward in the formalisms presented.
- ³⁶C. Pellegrini, J. Flick, I. V. Tokatly, H. Appel, and A. Rubio, *Phys. Rev. Lett.* **115**, 093001 (2015).
- ³⁷Q. Su and J. H. Eberly, *Phys. Rev. A* **44**, 5997 (1991).
- ³⁸N. M. Hoffmann, L. Lacombe, A. Rubio, and N. T. Maitra, *J. Chem. Phys.* **153**, 104103 (2020).
- ³⁹C. Schäfer, M. Ruggenthaler, V. Rokaj, and A. Rubio, *ACS Photonics* **7**, 975 (2020).
- ⁴⁰A. Mandal, M. A. Taylor, B. M. Weight, E. R. Koessler, X. Li, and P. Huo, *Chem. Rev.* **123**, 9786 (2023).